AIP | Review of Scientific Instruments

Design of solid state neutral particle analyzer array for National Spherical Torus Experiment-Upgradea)

D. Liu, W. W. Heidbrink, K. Tritz, Y. B. Zhu, A. L. Roquemore, and S. S. Medley

Citation: Review of Scientific Instruments **85**, 11E105 (2014); doi: 10.1063/1.4889913
View online: http://dx.doi.org/10.1063/1.4889913
View Table of Contents: http://scitation.aip.org/content/aip/journal/rsi/85/11?ver=pdfcov
Published by the AIP Publishing

Design of solid state neutral particle analyzer array for National Spherical Torus Experiment-Upgrade[a)]

D. Liu,[1,b)] W. W. Heidbrink,[1] K. Tritz,[2] Y. B. Zhu,[1] A. L. Roquemore,[3] and S. S. Medley[3]
[1]*Department of Physics and Astronomy, University of California - Irvine, Irvine, California 92697, USA*
[2]*Department of Physics and Astronomy, Johns Hopkins University, Baltimore, Maryland 21218, USA*
[3]*Princeton Plasma Physics Laboratory, Princeton, New Jersey 08543, USA*

(Presented 3 June 2014; received 1 June 2014; accepted 30 June 2014; published online 18 July 2014)

A new compact, multi-channel Solid State Neutral Particle Analyzer (SSNPA) diagnostic based on silicon photodiode array has been designed and is being fabricated for the National Spherical Torus Experiment-Upgrade (NSTX-U). The SSNPA system utilizes a set of vertically stacked photodiode arrays in current mode viewing the same plasma region with different filter thickness to obtain fast temporal resolution (∼120 kHz bandwidth) and coarse energy information in three bands of >25 keV, >45 keV, and >65 keV. The SSNPA system consists of 15 radial sightlines that intersect existing on-axis neutral beams at major radii between 90 and 130 cm, 15 tangential sightlines that intersect new off-axis neutral beams at major radii between 120 and 145 cm. These two subsystems aim at separating the response of passing and trapped fast ions. In addition, one photodiode array whose viewing area does not intersect any neutral beams is used to monitor passive signals produced by fast ions that charge exchange with background neutrals. © *2014 AIP Publishing LLC*. [http://dx.doi.org/10.1063/1.4889913]

I. INTRODUCTION

Neutral Particle Analyzer (NPA) diagnostics measure charge exchange neutral particle flux escaping from the plasma and provide valuable information on bulk ion temperature, plasma isotope composition, and fast ion distribution function, which are important for the control of the tritium/deuterium (T/D) density ratio in ITER[1] and the study of fast ion confinement and transport in Tokamak experiments.[2] In contemporary magnetic confinement devices, a variety of NPAs have been developed and deployed based on different re-ionization techniques and spectrometer design, including electrostatic, E‖B type and time-of-flight spectrometers.[3] Although conventional NPAs, for example, E‖B type NPA, can accurately measure the energy and distinguish incident particle mass, they are relatively large, expensive, and complicated, which make it impractical to build a compact and multi-channel system. As an alternative approach, solid state neutral particle analyzers (SSNPA) based on natural diamond detectors or silicon photodiodes are very attractive because of their compact size, low cost, and easy handling features, and they have been successfully demonstrated on TFTR,[4] LHD,[5–7,10] CHS,[8] NSTX,[9,11,12] Alcator C-mod,[13] and DIII-D.[14] It is worthy to note that the absolute extreme ultraviolet (AXUV) silicon photodiodes[15] from Opto Diode Corporation (formerly International Radiation Detectors, Inc.) have been widely implemented in soft x-ray, bolometric, and NPA diagnostics since the detectors have high responsivity, fast rise time, and ultra-high vacuum compatibility.

In NSTX, the SSNPA system based on four individual AXUV photodiodes was operated in pulse-counting mode in 2004–2009 run campaign, and later was switched to current mode in 2009–2011 run campaign. It had obtained useful data in both operational modes. In pulse-counting mode, each neutral creates a pulse of charge in the detector with pulse height proportional to the deposited energy. The pulse-counting mode provides an energy spectrum of neutral beam generated fast ions with ∼10 keV energy resolution and ∼2–10 ms time resolution.[12] Slowing down of fast ions after short neutral beam pulses was observed with the SSNPA.[16] In current mode, the SSNPA can measure fast ion density fluctuations with frequency up to ∼100 kHz by sacrificing energy resolution.[14] The main drawbacks of a silicon photodiode based SSNPA are that it cannot resolve the incident particle mass, and that soft x-ray and neutron/gamma ray induced noise could limit the performance in high density plasmas especially in pulse-counting mode. The NSTX Upgrade (NSTX-U) that is presently under construction will double the toroidal magnetic field and plasma current, and add off-axis neutral beam injection.[17] The existing SSNPA diagnostic was displaced from its original location and a new compact, multi-channel SSNPA system based on AXUV silicon photodiode arrays has been designed.

The new SSNPA system consists of a set of vertically stacked AXUV photodiode arrays in current mode with an overlapping view of the plasma near the midplane, which allows neutral particle measurements of the same plasma region with different filter thickness. This technique evolves from the successful operation of SSNPAs[14] in current mode on NSTX and DIII-D devices, and a multi-energy soft x-ray

[a)]Contributed paper, published as part of the Proceedings of the 20th Topical Conference on High-Temperature Plasma Diagnostics, Atlanta, Georgia, USA, June 2014.

[b)]Author to whom correspondence should be addressed. Electronic mail: deyongl@uci.edu.

(ME-SXR)[18] diagnostic on NSTX with AXUV photodiodes. One of the primary design goals of the new SSNPA diagnostic is to achieve fast time response with some energy information. This system will identify detailed physics mechanisms related to fast ion interactions with instabilities and complement the other existing fast-ion diagnostics on NSTX-U, which includes neutron detectors, a scintillator based fast ion loss probe (sFLIP), and two fast-ion *D*-alpha (FIDA) systems. In the rest of this paper, the design considerations and technical details are described, as well as the techniques to improve the signal to noise ratio.

II. DESIGN CONSIDERATIONS

Compared with other fast ion diagnostics, an NPA diagnostic has excellent pitch angle ($v_{\|}/v$) resolution. Tangential views are mainly sensitive to passing fast ions, while radial views are sensitive to trapped fast ions. A pair of tangential and radial views can help separate the response of passing and trapped fast ions. In addition, NPA signal is typically integrated along the line of sight and contains both "active" contributions from fast ions that charge exchange with beam neutrals in the intersection of the sightline and neutral beam, and "passive" contributions from fast ions that neutralize in the high neutral-density region near the plasma edge. Reference views that do not intersect any neutral beam could distinguish active and passive contributions and improve the NPA spatial localization. This is particularly important during high-density operation on NSTX-U, in which the active NPA signals strongly suffer from beam attenuation and additional signal loss due to reionization of the escaping neutrals during fly-out. Views in the midplane are more favorable than vertical views for high-density operation. Because NSTX-U plasmas are elongated, the longer path length of vertical NPA views limits the performance of NPA at high plasma density.

Based on the above considerations, the SSNPA system on NSTX-U is planned to consist of three subsystems near the equatorial plane: one tangential subsystem (t-SSNPA) at Bay I viewing the mid-radius plasmas, one nearly radial subsystem (r-SSNPA) at Bay L viewing the plasma core, and one passive reference subsystem (p-SSNPA) at Bay B (see Figure 1). The field of view of reference subsystem p-SSNPA only partially overlaps with that of r-SSNPA due to port size limitations. Figure 2 shows the pitch angels of t-SSNPA and r-SSNPA views calculated by the synthetic diagnostic code FIDAsim[19] are complementary to each other, as expected. The radial gradient of fast ion distribution is the main drive of Alfvén eigenmodes. It is desirable that the radial profile and its gradient of fast ion distribution can be measured experimentally. In the planned SSNPA system, a set of vertically stacked photodiode arrays, each array consisting of 16 elements, view the same plasma region with different filter thickness. With this approach, radial profile and coarse energy information of fast ion distribution can be obtained simultaneously.

III. TECHNICAL DESCRIPTION

The silicon photodiode arrays chosen for the SSNPA diagnostics on NSTX-U and EAST[20] are a modified version of

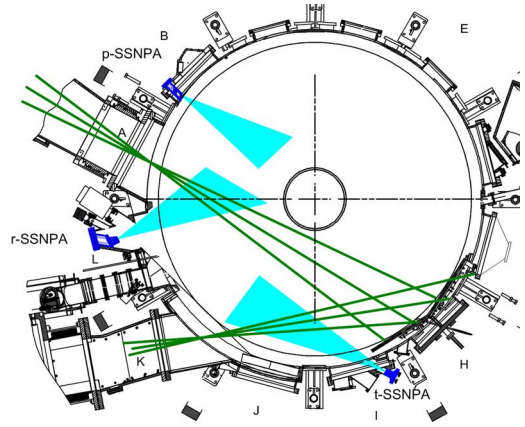

FIG. 1. Location and field view of the SSNPA diagnostic on NSTX-U. The solid green lines represent the centerlines of on-axis and off-axis neutral beamlines. The shaded light blue regions are the field of view of three SSNPA subsystems.

AXUV16ELG[15] from Opto Diode Corporation, in which the filters are directly deposited on the photodiodes. The photodiode array has sixteen 2 mm × 5 mm elements with a common anode and nominal capacitance of 2 nF. One apparent advantage is that directly deposited filters are more robust and reliable than free-standing foils. The filters are mainly composed of a tungsten layer, whose thickness can be 100, 200, or 300 nm, and the corresponding low energy thresholds for a deuteron are ~25, ~45, and ~65 keV, respectively, based on the simulation with Stopping and Range of Ions in Matter (SRIM) code.[21] Due to high atomic number, the tungsten filters effectively block visible light and low energy soft x-ray, but remain transparent to energetic neutrals. Similar filters were successfully used on the SSNPA on DIII-D[14] and a neutral particle bolometer in the C-2 experiment.[22] The photodiodes can be reverse-biased to 15–50V to decrease capacitance and thus decrease noise level.

The three SSNPA subsystems are very similar in hardware except that the reference subsystem p-SSNPA has only one photodiode array with 100 nm thick tungsten filter due to port size limitations, while the other two subsystems have three photodiode arrays with different filter thickness to provide energy resolution. Here, the hardware of the radial SSNPA subsystem r-SSNPA at Bay L is described for reference.

The SSNPA diagnostic is essentially a pinhole camera with one-dimensional silicon photodiode arrays. As shown in Fig. 3, the r-SSNPA is mounted to a D-shape vacuum interface, where four high density DB26 vacuum electrical feedthroughs are welded in. The in-vacuum hardware includes a set of AXUV16 photodiode arrays with different

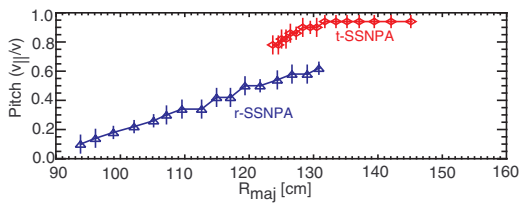

FIG. 2. Pitch angle of t-SSNPA and r-SSNPA views at the intersectional location of the sightline and neutral beam.

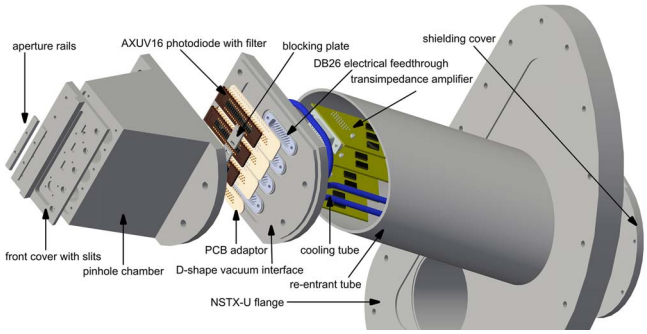

FIG. 3. Expanded view of SSNPA subsystem at Bay L. Shutter and enclosures for transimpdeance amplifiers are not shown.

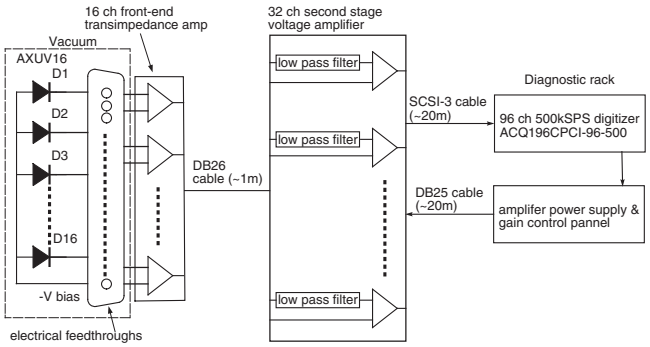

FIG. 4. Schematic diagram of the SSNPA electronics for one AXUV16 silicon photodiode array.

filter thickness, printed circuit board (PCB) adaptors, one pinhole chamber, front cover, and two aperture rails. The silicon photodiode arrays are plugged to the PCB adaptors made of low outgassing laminate Rogers 4003, and then are mounted to high density DB26 electrical feedthroughs. The photodiode arrays are housed inside the pinhole chamber, which has slits in the front cover. The internal buffers inside pinhole chamber optically isolate the photodiodes and prevent cross talk. Each photodiode array views the plasma through a separate aperture with an overlapping view of the same plasma region. The aperture rails sit on the top of the front cover and are ∼7 cm from the photodiode arrays. The aperture width is adjustable with aperture rails and is typically set to 8.5 mm × 3 mm, which gives radial resolution of 5 cm in the plasma core. The size and location of the apertures are optimized to achieve a good spatial coverage and spatial resolution. In addition, the viewing line of one edge element of each photodiode array is blocked to monitor electromagnetic (EM), and neutron/gamma ray induced noise, and thus noise can be subtracted from NPA signals. The inside of pinhole chamber, front cover, aperture rails, etc. are coated black to minimize light reflection.

A remotely controlled shutter is used to protect the photodiode arrays from lithium deposition during wall conditioning periods. It should be noted that, for the subsystems at Bay L and Bay B, vacuum interfaces are welded to re-entrant tubes in order to optimize viewing angle and make full use of available space. In addition, the vacuum interface is water cooled in order to keep the temperature of photodiode arrays below 150 °C during NSTX-U vessel bake-out. The cooling tubes are furnace brazed to the vacuum interface on the air side.

As shown in Fig. 4, the SSNPA electronics mainly consist of 16-channel transimpedance amplifiers, 32-channel 2nd stage voltage amplifiers, and a data acquisition system. The transimpedance amplifier based on MAZeT MTI04 integrated circuits (IC) is directly plugged to the electrical feedthrough on the atmosphere side to minimize the distance and capacitance between the detector and amplifier input, thereby improving the signal to noise ratio and signal bandwidth. The 2nd stage voltage amplifier adds another gain of 20 and provides a low output impedance to drive the analog voltage signal to the data acquisition system. The 2nd stage voltage amplifier also has built-in low pass filters with cutoff frequency of 300 kHz and the signal above 600 kHZ is attenuated by a factor of 10. This can prevent the SSNPA signals from high frequency electrostatic pickup, especially the ∼700 kHz noise from the switching power amplifiers (SPA) of resistive wall mode (RWM) coils.[16]

The signals after the amplifiers are transmitted by twisted-pair and double shielded SCSI-3 cables to D-Tacq digitizer ACQ196PCI-96–500. The digitizer supports 96 channels of 16-bit analog-to-digital conversion with sampling rate of 500 kHz and input voltage range of [−5, +5]V, and sends digital data directly to an MDSplus server. The digital input/output channels of the digitizer are used to control the amplifier gain. Besides the gain control, the SSNPA control panel uses a low noise linear regulated power supply to provide clean power to SSNPA amplifiers and a negative voltage bias to the AXUV photodiode arrays through a shielded and twisted pair DB25 cable. The gain and bandwidth of front-end transimpedance amplifier can be manually adjusted or remotely controlled via digital programming. Although the transimpedance amplifier has eight stages in gain/bandwidth adjustment, only two of them are planned to be used: 2.5 × 10^4 V/A with 300 kHz bandwidth and 1.0 × 10^5 V/A with 120 kHz bandwidth. The combination of front-end transmpedance amplifier and 2nd stage amplifier gives a total gain of 5 × 10^5 V/A or 2 × 10^6 V/A.

IV. FUTURE WORK

The combination of pulse-counting-mode and current-mode arrays will provide useful information on fast-ion density fluctuations and energy spectrum simultaneously. A detailed energy spectrum is crucial for the study of the acceleration of fast ions by Radio frequency (RF) waves. In the present design, AXUV silicon photodiodes work in current mode and provide only coarse energy information. However, one slot of the pinhole chamber for the radial and tangential subsystems is specially designed so that it can accommodate an additional photodiode array to work in pulse-counting mode. The main challenge for pulse-counting mode is to develop a compact, multi-channel, high gain and low noise charge sensitive amplifier, and integrate it with a fast shaping amplifier or buffer amplifier in order to obtain good energy resolution and high count rate. The SSNPA arrays that will work in pulse-counting mode are planned and the electronics are currently under development.

ACKNOWLEDGMENTS

The authors would like to thank A. Bortolon, D. S. Darrow, V. A. Soukhanovskii, and M. Podestá for helpful discussions and T. Kozub, L. Morris, and S. Z. Jurczynski for technical support. This work is supported by U.S. DOE under Grant Nos. DE-AC02-09CH11466, DE-FG02-06ER54867, and DE-FG03-02ER54681.

[1]ITER Technical Basis, *ITER EDA Documentation Series No. 24* (IAEA, Vienna, 2002).
[2]W. W. Heidbrink and G. J. Sadler, Nucl. Fusion **34**, 535 (1994).
[3]S. S. Medley, A. J. H. Donné, R. Kaita, A. I. Kislyakov, M. P. Petrov, and A. L. Roquemore, Rev. Sci. Instrum. **79**, 011101 (2008).
[4]A. V. Krasilnikov, S. S. Medley, N. N. Gorelenkov, R. V. Budny, O. V. Ignatyev, Yu A. Kaschuck, M. P. Petrov, and A. L. Roquemore, Rev. Sci. Instrum. **70**, 1107 (1999).
[5]M. Isobe *et al.*, Rev. Sci. Instrum. **72**, 611 (2001).
[6]M. Osakabe *et al.*, Rev. Sci. Instrum. **72**, 788 (2001).
[7]A. V. Krasilnikov *et al.*, Nucl. Fusion **42**, 759 (2002).
[8]T. Yamamoto *et al.*, Rev. Sci. Instrum. **72**, 615 (2001).
[9]A. G. Alekseyev, D. S. Darrow, A. L. Roquemore, S. S. Medley, V. N. Amosov, A. V. Krasilnikov, D. V. Prosvirin, and A. Yu. Tsutskikh, Rev. Sci. Instrum. **74**, 1905 (2003).
[10]J. F. Lyon, P. R. Goncharov, S. Murakami, T. Ozaki, D. E. Greenwood, D. A. Spong, and S. Sudo, Rev. Sci. Instrum. **74**, 1873 (2003).
[11]K. Shinohara, D. S. Darrow, A. L. Roquemore, S. S. Medley, and F. E. Cecil, Rev. Sci. Instrum. **75**, 3640 (2004).
[12]D. Liu, W. W. Heidbrink, D. S. Darrow, A. L. Roquemore, S. S. Medle, and K. Shinohara, Rev. Sci. Instrum. **77**, 10F113 (2006).
[13]V. Tang *et al.*, Rev. Sci. Instrum. **77**, 083501 (2006).
[14]Y. B. Zhu, A. Bortolon, W. W. Heidbrink, S. L. Celle, and A. L. Roquemore, Rev. Sci. Instrum. **83**, 10D304 (2012).
[15]See http://optodiode.com/products.html#IRD-UV-Photodiodes for more information about IRD AXUV silicon photodiode.
[16]D. Liu, "Fast-ion studies in the National Spherical Torus Experiment: Transport by instabilities and acceleration by high harmonic fast waves," Ph.D. thesis (University of California, 2009).
[17]J. E. Menard *et al.*, Nucl. Fusion **52**, 083015 (2012).
[18]K. Tritz, D. J. Clayton, D. Stutman, and M. Finkenthal, Rev. Sci. Instrum. **83**, 10E109 (2012).
[19]W. W. Heidbrink, D. Liu, Y. Luo, E. Ruskov, and B. Geiger, Commun. Comput. Phys. **10**, 716 (2011).
[20]Y. B. Zhu, J. Z. Zhang, M. Z. Qi, S. B. Xia, D. Liu, W. W. Heidbrink, B. N. Wan, and J. G. Li, "Development of an integrated energetic neutral particle measurement system on EAST full superconducting tokamak," Rev. Sci. Instrum. (these proceedings).
[21]J. Ziegler, J. Biersack, and U. Littmark, *The Stopping and Range of Ions in Solids* (Pergamon, 1985).
[22]R. Clary, A. Smirnov, S. Dettrick, K. Knapp, S. Korepanov, E. Ruskov, W. W. Heidbrink, and Y. Zhu, Rev. Sci. Instrum. **83**, 10D713 (2012).